PERGAMON

International Journal of Heat and Mass Transfer 45 (2002) 4227–4235

International Journal of HEAT and MASS TRANSFER

www.elsevier.com/locate/ijhmt

Stability of natural convection between spherical shells: energy theory

Vadim V. Travnikov [a,*], Hans J. Rath [b], Christoph Egbers [a]

[a] Department of Aerodynamics and Fluid Dynamics, BTU Cottbus, D-03046 Cottbus, Germany

[b] Center of Applied Space Technology and Microgravity, ZARM – University of Bremen, Am Fallturm, D-28359 Bremen, Germany

Received 9 March 2001; received in revised form 22 August 2001

Abstract

The energy stability problem with respect to axisymmetric disturbances of the natural convection in the narrow gap between two spherical shells under the earth gravity is discussed. The results are compared with the results of the linear stability analysis for the same problem. The problem is solved for different fluids with $Pr = 0$–100 and different radius ratios $\eta = 0.9, 0.925, 0.95$. With the aid of the variational principle Euler–Lagrange equations are received, which have the form of an eigenvalue problem, that is solved by means of Galerkin–Chebyshev spectral method. The convergence problem and the dependence of the critical stability parameter on Prandtl number are discussed. The calculations show that there is a big difference between critical numbers for energy and linear stability theories for the small Prandtl numbers. For large Prandtl numbers this difference is very small. © 2002 Published by Elsevier Science Ltd.

Keywords: Natural convection; Numerical methods; Stability

1. Introduction

In this article, the results of the energy stability theory of natural convection between spherical shells for Boussinesq fluids under the condition of earth gravity are presented. The two concentric spherical shells are maintained at constant, different temperatures. The inner sphere is warmer and maintained at a constant temperature T_1 while the outer sphere is at a constant temperature T_2. The gravity field acts antiparallel to the vertical axis. The geometry of system is presented in Fig. 1.

Stability analysis in the spherical geometry has been performed for different flows and boundary conditions. In [1,2] the flow between two rotating spheres was investigated with linear and energy stability theories, in [3,4] the spherical Rayleigh–Bénard problem was solved, in [5] the energy stability of Rayleigh–Bénard convection was investigated and in [6,7] the stability of the flow in the spherical gap for different gravity models.

The important experimental results for this kind of geometry were received in [8,9] for different η. The change of the flow as function of η and Rayleigh number for air and water [8] and silicone oil ($Pr = 100$) [9] was investigated. Detailed discussions of these results can be found in [10,12,13].

When the temperatures of two spheres are equal, there is no base flow. When the temperatures of two surfaces are different, buoyancy forces induce motion in the fluid between the spheres. The physics of the problem is more complicated than the usual Rayleigh–Bénard problem, because the gravity and temperature gradient are not always parallel and therefore the stability analysis is more difficult. The base flow depends on the geometry parameter $\eta = R_1/R_2$, the Prandtl number $Pr = \nu/k$ and the Rayleigh number $Ra = (g\alpha\Delta T\Delta R^3)/k\nu$. For narrow gaps $0.9 \leqslant \eta < 1$, for which we investigate the stability problem, this flow was analytically calculated by Wright and Douglas [11] and is discussed in Section 2. To investigate the stability of any flow, for example, two theories are used: linear and energy

* Corresponding author. Tel.: +49-355-69-5015; fax: +49-355-69-4891.

E-mail addresses: vadim.travnikov@las.tu-cottbus.de (V.V. Travnikov), rath@zarm.uni-bremen.de (H.J. Rath), egbers@las.tu-cottbus.de (C. Egbers).

0017-9310/02/$ - see front matter © 2002 Published by Elsevier Science Ltd.
PII: S0017-9310(02)00083-2

Nomenclature

$\vec{e}_r, \vec{e}_\vartheta$	unit vectors in radial and latitudinal directions
$\vec{e}_z$	$\cos\vartheta\vec{e}_r - \sin\vartheta\vec{e}_\theta$
$\hat{\Theta}$	disturbance temperature field
g	gravitational acceleration constant
$g_\ell(r), f_\ell(r)$	partial spectral
$h_\ell(r)$	functions
Gr	Grashof number, $g\alpha\Delta T\Delta R^3/\nu^2$
Pr	Prandtl number, ν/k
r	radial coordinate
z	radial coordinate, $r = \frac{1}{2}[z + \frac{1+\eta}{1-\eta}]$
$P_0, \hat{p}$	base flow, disturbance pressure
P	disturbed flow pressure
V	disturbed flow velocity
T	disturbed flow temperature
t	time
$\Re$	stability parameter, $\sqrt{Gr}$
Ra	Rayleigh number, $g\alpha\Delta T\Delta R^3/k\nu$
R_1, R_2	inner, outer radius of the spheres
ΔR	$R_2 - R_1$
T_n	Chebyshev polynomial of order n
P_n	Legendre polynomial of the first kind of degree n
Np	spherical harmonics truncation order
Nc	Chebyshev truncation order
$\Re_{cL}$	critical parameter of the linear stability theory
$\Re_{cE}$	critical parameter of the energy
T_0	base flow temperature field
T_1, T_2	inner, outer surface temperature
ΔT	$T_1 - T_2$
$\hat{v}_r, \hat{v}_\vartheta, \hat{v}_\varphi$	radial, latitudinal, longitudinal disturbance velocity
$V_{0r}, V_{0\theta}$	radial, latitudinal base flow velocity

Greek symbols

η	radius ratio R_1/R_2
ϵ	$1-\eta$, relative gap width
ν	kinematic viscosity
ϑ	latitudinal coordinate
x	$\cos\vartheta$
φ	longitudinal coordinate
σ	eigenvalue from linear theory
$\mathrm{Re}\{\sigma\}$	real part of σ
$\mathrm{Im}\{\sigma\}$	imaginary part of σ
ψ	base flow stream function
k	thermal diffusivity
$\hat{\Phi}, \hat{\Psi}$	poloidal and toroidal scalar functions
λ	Lagrange parameter
$\Gamma, \Delta, T_1, \Xi, \Omega$	functions describing the base flow
α	coefficient of volume expansion
$\Re_\lambda, \wp$	Lagrange coefficients
λ	energy parameter

stability theories. Both describe different aspects of the stability of the flow, therefore linear stability analysis as well as energy stability analysis are important for a detailed investigation of the flow stability. If the parameter $\Re = \sqrt{g\alpha\Delta T\Delta R^3/\nu^2}$ is larger than a critical value for a given Prandtl number and radius ratio, the flow is unstable. The linear theory gives this critical number and predicts the instability. We note this value $\Re_{cL}$. However, for $\Re < \Re_{cL}$, linear stability analysis is not enough to predict the behaviour of the system. To investigate the system for $\Re < \Re_{cL}$, the energy stability analysis is used to determine the critical value $\Re_{cE}$. If the stability parameter $\Re$ is smaller than $\Re_{cE}$, the flow is definitely stable. Necessarily, $\Re_{cE} \leqslant \Re_{cL}$. The stability problem for this flow in the frame of linear theory was investigated by Farmer et al. [10] and Gardner [12]. Because Farmer assumed that the principle of exchange of stability is valid for all Prandtl numbers and received results, which distinguish from Gardner's results, who solved the eigenvalue problem without this assumption. Indeed this principle exists only for some Prandtl numbers.

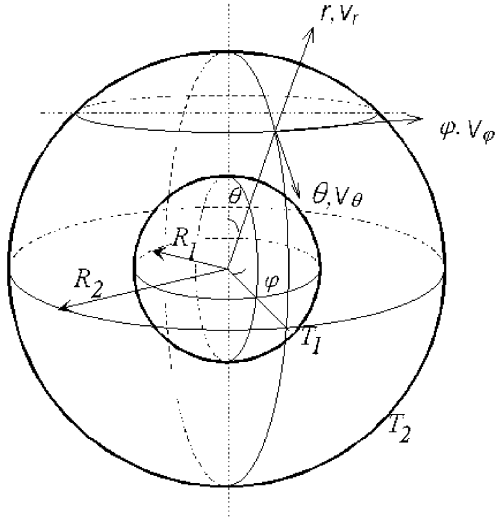

Fig. 1. Spherical geometry.

2. The base flow

To investigate the stability of the flow, the expression for the base flow must be received. The governing

equations [12] consist of the continuity equation, Navier–Stokes equation and the thermal energy equation with boundary conditions. Now we will non-dimensionalize all these equations due to following set of scales:

Length $\Delta R = R_2 - R_1$,

Temperature $\Delta T = T_2 - T_1$,

Velocity $V = \sqrt{g\alpha\Delta T\Delta R}$,

Time scale $t = L/V$,

Pressure scale $P = \rho V^2$.

Introducing this dimensionless variables the governing equation and boundary conditions are:

$$\frac{\partial \vec{V}_0}{\partial t} + (\vec{V}_0\nabla)\vec{V}_0 = -\nabla P_0 + T_0\vec{e}_z + \frac{1}{\Re}\Delta\vec{V}_0, \tag{1}$$

$$\frac{\partial T_0}{\partial t} + (\vec{V}_0\nabla)T_0 = \frac{1}{Pr\Re}\Delta T_0, \tag{2}$$

$$\nabla\vec{V}_0 = 0, \tag{3}$$

$$\begin{aligned} &T_0(\eta/\epsilon,\vartheta,\varphi) = 1,\\ &T_0(1/\epsilon,\vartheta,\varphi) = 0,\\ &\vec{V}_0(\eta/\epsilon,\vartheta,\varphi) = \vec{V}_0(1/\epsilon,\vartheta,\varphi) = 0. \end{aligned} \tag{4}$$

The problem expressed by this equations has an approximate, steady, axisymmetric base flow solution for small values of ϵ [11]. This solution can be expressed in the following form:

$$\psi(r,x) = (1-x^2)[\Gamma(r,\Re,Pr,\epsilon) + x\Delta(r,\Re,Pr,\epsilon)], \tag{5}$$

$$\begin{aligned} T_0(r,x) = T_1(r,Pr,\epsilon) + x[&\Xi(r;\Re,Pr,\epsilon)\\ &+ x\Omega(r;\Re,Pr,\epsilon)], \end{aligned} \tag{6}$$

where $\psi(r,x)$ is the stream function, T_0 is the temperature function, $x = \cos\vartheta$, $\Re = \sqrt{g\alpha\Delta T(\Delta R)^3/\nu^2}$ and the functions T_1, Γ, Δ, Ξ and Ω are given in [12].

This solution is valid for the radius ratios $0.9 \leqslant \eta < 1$ and for values of $\Re$ in the range $0 \leqslant \Re < \sqrt{720/\epsilon Pr}$.

The components of the velocity vector of the base flow is obtained from the stream function ψ by the relations:

$$V_{0r} = -\frac{1}{r^2}\frac{\partial\psi}{\partial x}, \quad V_{0\vartheta} = -\frac{1}{r\sqrt{1-x^2}}\frac{\partial\psi}{\partial r}, \quad V_{0\varphi} = 0. \tag{7}$$

3. Formulation of the problem

3.1. Linear stability analysis

Let $(\vec{\hat{v}}(r,x,\varphi,t), \hat{\Theta}(r,x,\varphi,t), \hat{p}(r,x,\varphi,t))$ be a small disturbance of the base flow. If we substitute the sum of the base flow and the disturbance flow

$$\vec{V} = \vec{V}_0 + \vec{\hat{v}},$$

$$T = T_0 + \hat{\Theta},$$

$$P = P_0 + \hat{p}$$

in the governing equations (1)–(3) and use that $(\vec{V}_0, T_0, P_0)$ is a solution of them, we obtain the system of equations for the perturbations:

$$\begin{aligned} &\frac{\partial\vec{\hat{v}}}{\partial t} + (\vec{\hat{v}}\nabla)\vec{V}_0 + (\vec{V}_0\nabla)\vec{\hat{v}} + (\vec{\hat{v}}\nabla)\vec{\hat{v}}\\ &\quad = -\nabla\hat{p} + \hat{\Theta}\vec{e}_z + \frac{1}{\Re}\Delta\vec{\hat{v}}, \end{aligned} \tag{8}$$

$$\frac{\partial\hat{\Theta}}{\partial t} + \vec{\hat{v}}\nabla T_0 + \vec{V}_0\nabla\hat{\Theta} + \vec{\hat{v}}\nabla\hat{\Theta} = \frac{1}{\Re Pr}\Delta\hat{\Theta}, \tag{9}$$

$$\nabla\vec{\hat{v}} = 0 \tag{10}$$

with boundary conditions

$$\begin{aligned} &\hat{\Theta}(\eta/\epsilon,\vartheta,\varphi) = \hat{\Theta}(1/\epsilon,\vartheta,\varphi) = 0,\\ &\hat{v}(\eta/\epsilon,\vartheta,\varphi) = \hat{v}(1/\epsilon,\vartheta,\varphi) = 0. \end{aligned} \tag{11}$$

We seek the solution of the problem in the following form:

$$\vec{\hat{v}}(r,x,\varphi,t) = \vec{\hat{v}}_0(r,x,\varphi)e^{\sigma t},$$

$$\hat{\Theta}(r,x,\varphi,t) = \hat{\Theta}_0(r,x,\varphi)e^{\sigma t},$$

$$\hat{p}(r,x,\varphi,t) = \hat{p}_0(r,x,\varphi)e^{\sigma t}.$$

After the substitution of this expressions in (8)–(10) and neglecting the nonlinear terms we receive the linear stability equations which form a eigenvalue problem for σ. To calculate the critical stability parameter for the linear theory $\Re_{cL}$ we have to calculate the eigenvalue with $Re(\sigma) = 0$. The imaginary part of the eigenvalue is important, too. If the imaginary part is zero the *Principle of Exchange of Stabilities* is valid and the bifurcation is steady, otherwise we have a time-periodic bifurcation. Only numerical research and the solution of the eigenvalue problem can answer the question about kind of bifurcation. The details about linear stability analysis can be found in [12,13] and in the results of this article.

3.2. Energy stability analysis

The main contribution in the energy stability theory for hydrodynamic problems was made by Serrin [14] and Joseph [15].

In the global stability theory energy methods play an important role, because they define a criterion, which is sufficient for the global stability of the basic flow.

To formulate Euler–Lagrange equations we use Eqs. (8)–(10) with boundary conditions and the method of calculus of variations.

Introducing an *energy*

$$E_\lambda = E_{\text{kin.}} + \lambda E_{\text{therm.}}, \tag{12}$$

where

$$E_{\text{kin.}} = \frac{1}{2}\int \hat{v}^2\,\mathrm{d}V, \quad E_{\text{therm.}} = \frac{1}{2}Pr\int \hat{\Theta}^2\,\mathrm{d}V \tag{13}$$

with positive λ and the notations

$$I_1 = \int [\vec{\hat{v}}D\vec{\hat{v}} - \hat{\Theta}(\vec{\hat{v}}\vec{e}_z)]\,\mathrm{d}V, \quad I_2 = \int [\hat{\Theta}\vec{\hat{v}}\nabla T_0]\,\mathrm{d}V,$$

$$D_1 = \int [\nabla\hat{v} : \nabla\hat{v}]\,\mathrm{d}V, \quad D_2 = \int (\nabla\hat{\Theta})^2\,\mathrm{d}V,$$

$$I_\lambda = I_1 + \lambda PrI_2, \quad D_\lambda = D_1 + \lambda D_2, \tag{14}$$

where

$$D_{ij} = \frac{1}{2}\left(\frac{\partial V_{0i}}{\partial x_j} + \frac{\partial V_{0j}}{\partial x_i}\right), \tag{15}$$

we can write

$$\frac{1}{D_\lambda}\frac{\mathrm{d}E_\lambda}{\mathrm{d}t} = -\frac{1}{\Re} - \frac{I_\lambda}{D_\lambda} \leqslant -\frac{1}{\Re} + \frac{1}{\rho_\lambda}, \tag{16}$$

where

$$\rho_\lambda^{-1} = \max_{\mathbb{H}}\left(-\frac{I_\lambda}{D_\lambda}\right). \tag{17}$$

Here $\mathbb{H}$ is the collection of smooth functions satisfying $\nabla\vec{\hat{v}} = 0$ and boundary conditions (11).

Joseph has shown that [5]

$$E_\lambda(t) \leqslant E_\lambda(0)\exp\left[-\xi^2\left(\frac{1}{\Re} - \frac{1}{\rho_\lambda}\right)t\right]. \tag{18}$$

Stability is guaranteed if $\Re < \rho_\lambda$. This leads to the idea to formulate the maximum problem for the number $1/\rho_\lambda$. The calculation of the maximum of this number is equivalent to the calculation of the maximum of the expression

$$-\frac{I_\lambda}{D_\lambda} = \frac{-I_1(\vec{\hat{v}},\hat{\Theta}) - \lambda PrI_2(\vec{\hat{v}},\hat{\Theta})}{D_1(\vec{\hat{v}},\vec{\hat{v}}) + \lambda D_2(\hat{\Theta},\hat{\Theta})}. \tag{19}$$

For following calculations the maximum problem is formulated in the frames of variational calculus. The functional is defined on solenoidal vector fields. We have the variational problem (17) with boundary conditions (11), continuity equation (10) and normalizing condition

$$D_1(\vec{\hat{v}},\vec{\hat{v}}) + \lambda D_2(\hat{\Theta},\hat{\Theta}) = 1. \tag{20}$$

Writing the variational principle in the form

$$\delta J = 0, \tag{21}$$

where

$$J = I_1 + \lambda PrI_2 - \frac{2}{\Re_\lambda}\int \wp\nabla\vec{\hat{v}}\,\mathrm{d}V + \frac{1}{\Re_\lambda}(D_1 + \lambda D_2), \tag{22}$$

and $\wp(z,x,\varphi)$ and $\Re_\lambda$ are Lagrange coefficients resulting from the normalization condition (20) and the condition $\nabla\vec{\hat{v}} = 0$, we can write the Euler–Lagrange equations, corresponding to (22),

$$\Re_\lambda(D\vec{\hat{v}}) + \frac{1}{2}\Re_\lambda Pr\lambda(\nabla T_0\hat{\Theta}) - \frac{1}{2}\Re_\lambda\vec{e}_z\hat{\Theta} = -\nabla\wp + \Delta\vec{\hat{v}}, \tag{23}$$

$$\frac{1}{2}\Re_\lambda Pr(\vec{\hat{v}}\nabla T_0) - \frac{1}{2}\frac{\Re_\lambda}{\lambda}\vec{\hat{v}}\vec{e}_z = \Delta\hat{\Theta} \tag{24}$$

with boundary conditions (11).

Here

$$\vec{e}_z = \cos\vartheta\vec{e}_r - \sin\vartheta\vec{e}_\vartheta. \tag{25}$$

The base flow is axisymmetric and therefore the matrix D_{ij} has the form

$$D_{ij} = \begin{pmatrix} D_{11} & D_{12} & 0 \\ D_{21} & D_{22} & 0 \\ 0 & 0 & D_{33} \end{pmatrix}.$$

From Eqs. (23) and (24) the following expression for ρ_λ^{-1} can be written:

$$\max(-I_\lambda) = \max\left(\frac{1}{\Re_\lambda}\right) = \frac{1}{\rho_\lambda}$$

or

$$\rho_\lambda = \min(\Re_\lambda). \tag{26}$$

For the critical eigenvalue from the energy theory we have the following expression:

$$\Re_{\text{cE}} = \max_\lambda \min\Re_\lambda. \tag{27}$$

The λ number maximizing ρ_λ we call λ_{best}. This number can be calculated using [5]

$$\lambda_{\text{best}} = \frac{\int_V \vec{\hat{v}}\vec{e}_z\Theta\,\mathrm{d}V}{Pr\int_V(\vec{\hat{v}}\nabla T_0)\Theta\,\mathrm{d}V}. \tag{28}$$

Eqs. (23) and (24) with boundary conditions (11) must be solved.

4. Solution of the problem

4.1. Equations for energy stability analysis

Since according to the continuity equation $\operatorname{div}\vec{\hat{v}} = 0$, $\vec{\hat{v}}$ is a solenoidal vector, it is possible to express the disturbance velocity as a sum of two velocities which depends from two scalar potentials

$$\vec{\hat{v}} = \vec{\hat{v}}_1 + \vec{\hat{v}}_2, \tag{29}$$

where

$$\vec{\hat{v}}_1 = \mathrm{rotrot}(\hat{\Phi}\vec{r}), \quad \vec{\hat{v}}_2 = \mathrm{rot}(\hat{\Psi}\vec{r}). \tag{30}$$

The scalar functions $\hat{\Phi}(r,x,\varphi)$ and $\hat{\Psi}(r,x,\varphi)$ are the poloidal and toroidal potentials. Our goal is to express the equations for disturbance flow with the boundary conditions in terms of these potentials.

For the velocity components we have following expressions:

$$\hat{v}_r = -\frac{1}{r}\nabla_s^2\hat{\Phi}, \tag{31}$$

$$\hat{v}_\vartheta = \frac{1}{\sqrt{1-x^2}}\frac{\partial\hat{\Psi}}{\partial\varphi} - \frac{\sqrt{1-x^2}}{r}\frac{\partial}{\partial r}\left(r\frac{\partial\hat{\Phi}}{\partial x}\right), \tag{32}$$

$$\hat{v}_\varphi = \sqrt{1-x^2}\frac{\partial\hat{\Psi}}{\partial x} + \frac{1}{r\sqrt{1-x^2}}\frac{\partial}{\partial r}\left(r\frac{\partial\hat{\Phi}}{\partial\varphi}\right), \tag{33}$$

where

$$\nabla_s^2(\cdot) = \frac{\partial}{\partial x}\left[(1-x^2)\frac{\partial(\cdot)}{\partial x}\right] + \frac{1}{1-x^2}\frac{\partial^2(\cdot)}{\partial\varphi^2}. \tag{34}$$

The system (23) and (24) can now be solved using the method of normal modes and orthogonality properties of toroidal and poloidal fields.

Let $A(r,x,\varphi)$ represent an arbitrary function, that can be expanded as

$$A(r,x,\varphi) = \sum_{\ell=0}^{\infty}\sum_{m=-\ell}^{\ell} a_{\ell m}(r)Y_\ell^m(x,\varphi), \tag{35}$$

where the functions

$$Y_\ell^m(x,\varphi) = \left[\frac{2\ell+1}{4\pi}\frac{(\ell-m)}{(\ell+m)}\right]^{1/2} P_\ell^m(x)\mathrm{e}^{\mathrm{i}m\varphi} \tag{36}$$

are the spherical harmonics. They have the following orthogonality property:

$$\int_{-1}^{1}\int_0^{2\pi} \bar{Y}_\ell^m(x,\varphi)Y_k^n(x,\varphi)\,\mathrm{d}\varphi\,\mathrm{d}x = \delta_{\ell k}\delta_{mn}. \tag{37}$$

We write the series for $\hat{\Phi}$, $\hat{\Psi}$ and $\hat{\Theta}$ as

$$\hat{\Phi}(r,x,\varphi) = \sum_{\ell=1}^{\mathrm{Np}}\sum_{m=-\ell}^{\ell} g_{\ell m}(r)P_\ell^m(x)\mathrm{e}^{\mathrm{i}m\varphi}, \tag{38}$$

$$\hat{\Psi}(r,x,\varphi) = \sum_{\ell=1}^{\mathrm{Np}}\sum_{m=-\ell}^{\ell} f_{\ell m}(r)P_\ell^m(x)\mathrm{e}^{\mathrm{i}m\varphi}, \tag{39}$$

$$\hat{\Theta}(r,x,\varphi) = \sum_{\ell=0}^{\mathrm{Np}-1}\sum_{m=-\ell}^{\ell} h_{\ell m}(r)P_\ell^m(x)\mathrm{e}^{\mathrm{i}m\varphi}, \tag{40}$$

where the infinite sum has been truncated to Np terms and the unknown set of functions $g_{\ell m}(r)$, $f_{\ell m}(r)$ and $h_{\ell m}(r)$. P_ℓ^m are the associated Legendre functions.

To receive the equations of the functions $\hat{\Phi}$, $\hat{\Psi}$ and $\hat{\Theta}$ we use the properties of poloidal and toroidal fields.

To eliminate $\nabla\wp$, the operator curl is applied to both parts of Eq. (23). Now we can rewrite this equation as follows:

$$\begin{aligned}-\mathrm{curl}^3\vec{\hat{v}} &= -\mathrm{curl}(\vec{r}\nabla^4\hat{\Phi}) + \mathrm{curl}^2(\vec{r}\nabla^2\hat{\Psi})\\ &= \mathrm{curl}\left(\Re_\lambda(D\vec{\hat{v}}) + \frac{1}{2}\Re_\lambda Pr\lambda(\nabla T_0\hat{\Theta}) - \frac{1}{2}\Re_\lambda\vec{e}_z\hat{\Theta}\right)\end{aligned} \tag{41}$$

Now we will introduce new poloidal and toroidal fields:

$$S_r = -\frac{1}{r^2}\nabla_s^2 Y_\ell^m(\vartheta,\varphi), \quad S_\vartheta = 0, \quad S_\varphi = 0, \tag{42}$$

$$\begin{aligned}&T_r = 0, \quad T_\vartheta = \frac{1}{\sin\theta}\frac{\partial Y_\ell^m(\vartheta,\varphi)}{\partial\varphi},\\ &T_\varphi = -\frac{\partial Y_\ell^m(\vartheta,\varphi)}{\partial\vartheta}.\end{aligned} \tag{43}$$

To receive the equations for function $\hat{\Phi}$ we have to calculate the scalar product of the expressions (41) and (43); for function $\hat{\Psi}$ we calculate the scalar product of (41) and (42). The system of the differential equations for $\hat{\Phi}$, $\hat{\Psi}$ and $\hat{\Theta}$ can be written in the form of an eigenvalue problem

$$Ax = \Re_\lambda Bx, \tag{44}$$

here

$$A = \begin{pmatrix}\nabla^4\nabla_s^2 & 0 & 0\\ 0 & \nabla^2\nabla_s^2 & 0\\ 0 & 0 & \nabla^2\end{pmatrix},$$

where

$$x = \begin{pmatrix}\hat{\Phi}\\ \hat{\Psi}\\ \hat{\Theta}\end{pmatrix}$$

is the eigenvector and $\Re_\lambda$ the eigenvalue of the energy stability problem. The matrix B is much more complicated and the coefficients B_{ij} can be obtained after a lot of calculations.

If we substitute the expressions (38)–(40) in this equations and use the orthogonality properties of Legendre polynomials we receive a finite set of ordinary differential equations for the functions $g_{\ell m}$, $f_{\ell m}$ and $h_{\ell m}$. These equations are available, on request, from the authors.

Before we apply the Galerkin–Chebyshev spectral method, we have to map the radial coordinate from domain $[\eta/\epsilon, 1/\epsilon]$ onto a domain $[-1,1]$, where the Chebyshev polynomials are defined, using the following expression:

$$r = \frac{1}{2}\left[z + \frac{1+\eta}{1-\eta}\right]. \tag{45}$$

Table 1
Convergence analysis

Pr	$\eta = 0.9$				$\eta = 0.925$				$\eta = 0.95$			
	Energy Theory		Linear Theory		Energy Theory		Linear Theory		Energy Theory		Linear Theory	
	Nc	Np	Nc	Np	Nc	Np	Nc	Np	Nc	Np	Nc	Np
0.26–0.29	12	60	12	55	12	90	12	60		$\gg 90$		$\gg 60$
0.3	12	55	12	50	12	55	12	55		$\gg 55$		$\gg 55$
0.7–100	8	45	8	45	8	55	8	50	8	75	8	75

Now the functions $g_{\ell m}$ and $h_{\ell m}$ (we consider the energy stability problem with respect to axialsymmetric disturbances) can be expanded in a truncated series of Chebyshev polynomials. For example,

$$g^{(\mathrm{IV})}_{\ell m}(z) = \sum_{k=0}^{\mathrm{Nc}} a_{\ell k m} T_k(z), \tag{46}$$

$$h^{(\mathrm{II})}_{\ell m}(z) = \sum_{k=0}^{\mathrm{Nc}} b_{\ell k m} T_k(z), \tag{47}$$

where $T_k(z)$ are Chebyshev polynomial $T_k(z) = \cos[k \arccos(z)]$ with following orthogonality properties:

$$\int_{-1}^{1} \frac{T_m(z) T_n(z)}{\sqrt{1-z^2}}\,\mathrm{d}z = c_n \pi \delta_{mn}/2, \tag{48}$$

$c_0 = 2, \quad c_n = 1 \;\; n \geqslant 1.$

For other derivatives we have the following expressions:

$$g^{(\beta)}_{\ell m}(z) = \sum_{j=0}^{\mathrm{Nc}+4-\beta} \sum_{k=0}^{\mathrm{Nc}} g^{(\beta)}_{jk} a_{\ell k m} T_j(z) \tag{49}$$

for $\beta = 0, 1, 2, 3,$

$$h^{(\beta)}_{\ell m}(z) = \sum_{j=0}^{\mathrm{Nc}+2-\beta} \sum_{k=0}^{\mathrm{Nc}} h^{(\beta)}_{jk} b_{\ell k m} T_j(z) \tag{50}$$

for $\beta = 0, 1, 2.$

The coefficients $g^{(\beta)}_{jk}, h^{(\beta)}_{jk}$ are presented in [16].

Substituting this series in (44) we receive the eigenvalue problem for coefficients $a_{\ell k m}$ and $b_{\ell k m}$.

The elements of matrices A and B depend on the physical and geometrical parameters of the problem ϵ, Pr and $\mathfrak{R}$ and the numerical parameters Nc and Np (sufficiently high values of Nc and Np are required for convergence). The eigenvalues were computed using the commercial NAG routines.

4.2. Algorithm of solution

To receive the critical stability parameter for energy theory we have to calculate

$$\mathfrak{R}_{\mathrm{cE}} = \max_{\lambda} \min \mathfrak{R}_{\lambda}.$$

This critical parameter produce a surface of stability of the form

$$\mathfrak{R}_{\mathrm{cE}} = \mathfrak{R}_{\mathrm{cE}}(\eta, Pr; \mathrm{Nc}, \mathrm{Np}).$$

The solution procedure to find $\mathfrak{R}_{\mathrm{cE}}$ is represented in the following algorithm:

1. Fix the geometry of the system η $(0.9 \leqslant \eta < 1)$.
2. Select a value of the Prandtl number, Pr, fixing the fluid to be used.
3. Select a value of $\mathfrak{R}$.
4. Fix λ.
5. Compute the elements of matrices A and B.
6. Calculate eigenvalues and find smallest positive eigenvalue $\mathfrak{R}_{\lambda}$.
7. If $\mathfrak{R}_{\lambda} = \mathfrak{R}$ then go to step 8.
   If $\mathfrak{R}_{\lambda} < \mathfrak{R}$ then decrement $\mathfrak{R}$, if $\mathfrak{R}_{\lambda} > \mathfrak{R}$ then increment $\mathfrak{R}$ (step 3).
8. The steps 4–7 must be done for different λ. We receive the function $\mathfrak{R}_{\lambda}(\lambda)$. And we find $\max_{\lambda>0} \mathfrak{R}_{\lambda}$. We denote λ, that gives maximum for this function, as λ_0.
9. Calculate eigenvector for λ_0 and disturbance velocity and temperature fields, substitute in the expression (28) and calculate λ_{new}.
   If $\lambda_{\mathrm{new}} \neq \lambda_0$, then repeat steps 4–7 for λ_{new}. If $\lambda_{\mathrm{new}} = \lambda_0$, then $\mathfrak{R}_{\mathrm{cE}}$ is calculated.
10. Repeat steps 3–8 for different combinations of η and Pr.
11. The convergence analysis must be performed.

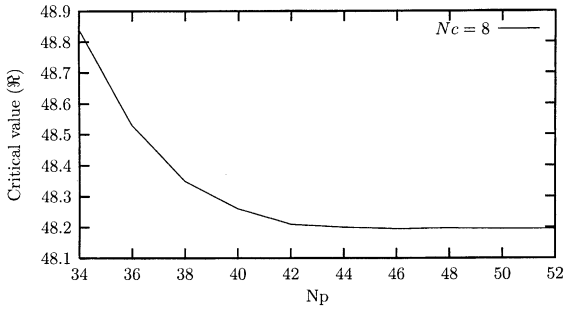

Fig. 2. Convergence curve for $\eta = 0.9$ and $Pr = 0.7$.

Table 2
Critical eigenvalues for Prandtl numbers near Pr_t

Pr	$\eta = 0.9$	Pr	$\eta = 0.925$
	σ		σ
0.25	$9.7013 \times 10^{-5} + i11.6439$	0.25	$8.1503 \times 10^{-4} + i8.6067$
0.26	$2.4114 \times 10^{-4} + i11.6098$	0.26	$-6.0123 \times 10^{-4} + i8.5972$
0.27	$1.7510 \times 10^{-5} + i11.5858$	0.27	$5.8920 \times 10^{-4} + i8.5911$
0.28	$5.4239 \times 10^{-5} + i11.5772$	0.28	$-5.2291 \times 10^{-4} + i0.0$
0.29	$-8.2666 \times 10^{-4} + i0.0$	0.29	$-1.4118 \times 10^{-4} + i0.0$
0.30	$6.080214 \times 10^{-4} + i0.0$	0.30	$3.3564 \times 10^{-4} + i0.0$
0.31	$5.9650 \times 10^{-4} + i0.0$	0.31	$6.5983 \times 10^{-6} + i0.0$

5. Convergence analysis

The solution of the problem depends not only on parameters η, Pr and $\Re$, but also on numerical Chebyshev and Legendre truncation orders Nc and Np. Nc controls the number of Chebyshev polynomials used in the radial direction of the disturbances and Np the number of Legendre polynomials used in the latitudinal variation of the disturbances.

For any radius ratio and Prandtl number the convergence has to be checked, because the calculations show that the convergence depends essentially on this truncation orders. In Table 1 the numbers Nc and Np necessary for the convergence are presented.

The convergence analysis is compared for both stability theories linear and energy.

In Fig. 2 the convergence analysis for $\eta = 0.9$ and $Pr = 0.7$ for linear theory is shown. The dependence of the necessary truncation orders on the radius ratio is summarized in Table 1.

From the convergence analysis we can draw the following conclusions:

1. To receive convergence we need the same Chebyshev polynomials number for both theories.
2. But we need more Legendre polynomials to receive the convergence for the energy stability theory than for linear theory.
3. The narrower gap, the more Legendre polynomials must be considered. For small Prandtl numbers a very large number of Legendre polynomials are needed.
4. The stability curves are similar for both stability theories.

6. Results and discussions

Stability investigations have been done for $\eta = 0.9$, $\eta = 0.925$ and $\eta = 0.95$. The Prandtl number was varied from 0 to 100 to compare the results with [12]. The results are presented in the form of a table and diagrams where the critical stability parameter $\Re = \sqrt{Gr}$ for energy and linear stability analysis are compared.

Although we have calculated the stability problem with respect to axisymmetric disturbances for all Prandtl numbers $Pr = 0$–100 very detailed, the three dimensional analysis for the linear and energy stability theories shows that $m = 0$ is the critical mode for $Pr = 0.1$ and $Pr = 0.7$ for $\eta = 0.9$ and $\eta = 0.925$ (Table 4). Here we have differences between our results and Gardner's results [12]: for $Pr = 0.7$ he found a critical mode with wave number $m = 2$. Generally, the critical numbers in [12] are higher then in our paper. The difference increases from 0.2% for small Prandtl numbers to 7.5% for large Prandtl numbers. The reason for this difference is not clear, but for narrow gap our results are very close to $Ra = 1708$ from the analytical results for the plane Rayleigh–Bénard stability problem. For example for $\eta = 0.95$, $Pr = 0.7$ we get $Ra_{cL} = 1699.96$ and in [12] $Ra_{cL} = 1771$.

The kind of the bifurcation depends on the Prandtl number [12,13]. If the imaginary part of the eigenvalue is zero ($\mathrm{Im}(\sigma) = 0$), then we deal with a steady bifurcation and the *Principle of Exchange of Stabilities* is valid. If a imaginary part of the eigenvalue is not zero, then we deal with a time-periodic bifurcation or the Hopf bifurcation of the basic flow. The boundary Prandtl number between this kinds of bifurcation is defined as *transition Prandtl number*, Pr_t.

In the frames of the linear theory we have calculated the transition Prandtl number as in [12] for $\eta = 0.9$ and $\eta = 0.925$, too. For $\eta = 0.95$ it is unfortunately very complicated because we need much more Legendre polynomials for that. The stability curve near the transition

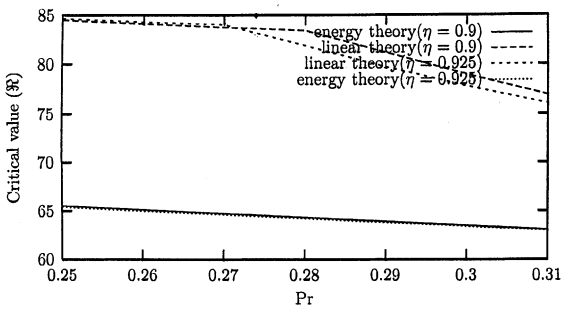

Fig. 3. Stability curve near Pr_t.

Table 3
Critical numbers $\Re$ for linear and energy stability theories

Pr	$\eta = 0.9$			$\eta = 0.925$			$\eta = 0.95$		
	λ_{best}	$\Re_{cE}$	$\Re_{cL}$	λ_{best}	$\Re_{cE}$	$\Re_{cL}$	λ_{best}	$\Re_{cE}$	$\Re_{cL}$
0.0			108.92			104.834			
0.1	8.83	71.47	94.606	8.79	71.28	91.728			
0.2	4.74	67.55	87.24	4.73	67.40	87.028			
0.25	3.89	65.54	84.517	3.89	65.42	84.643			
0.26	3.76	65.13	84.103	3.75	65.0	84.3			
0.27	3.63	64.72	83.732	3.63	64.62	84.005			
0.28	3.52	64.32	83.403	3.51	64.22	81.843			
0.29	3.40	63.91	81.167	3.40	63.82	79.683			
0.3	3.30	63.49	78.94	3.30	63.42	77.795			
0.31	3.20	63.08	76.935	3.20	63.02	76.046			
0.4	2.49	59.31	65.022	2.52	59.417	65.31			
0.5	1.91	54.97	57.445	2.0	55.43	58.002			
0.7	1.2792	46.8766	48.197	1.3391	47.7914	48.814	1.3932	48.5650	49.28
1.0	0.8873	39.2752	40.196	0.9296	40.0624	40.767	0.9663	40.7395	41.20
6.0	0.1462	16.0417	16.36	0.1537	16.3708	16.613	0.1602	16.6578	16.807
10.0	0.0877	12.4255	12.672	0.0922	12.6808	12.865	0.096	12.9038	13.02
15.0	0.0584	10.1452	10.345	0.0614	10.3538	10.507	0.064	10.5361	10.63
20.0	0.0438	8.7859	8.96	0.046	8.9666	9.097	0.048	9.1246	9.206
30.0	0.0292	7.1736	7.315	0.03	7.3208	7.43	0.032	7.4503	7.52
40.0	0.0219	6.2125	6.33	0.023	6.3404	6.43	0.024	6.4522	6.51
50.0	0.0175	5.5566	5.665	0.0184	5.6709	5.75	0.0192	5.7710	5.82
60.0	0.01459	5.0724	5.17	0.0153	5.1769	5.25	0.016	5.2682	5.31
70.0	0.01251	4.6961	4.79	0.01316	4.7928	4.86	0.0137	4.8774	4.92
80.0	0.0109	4.3928	4.48	0.0115	4.4833	4.546	0.012	4.5624	4.60
90.0	0.00973	4.1416	4.23	0.01	4.2266	4.28	0.0106	4.3015	4.34
100.0	0.0087	3.92904	4.0	0.0092	4.01	4.06	0.0096	4.0807	4.12

Prandtl number is presented in Fig. 3. Together with results for linear stability theory the results for energy stability theory for small Prandtl numbers are shown.

In Table 2 the dependence of the kind of bifurcation (Hopf or steady) on the Prandtl number can be observed. The real part is not exactly zero but numerically. All the critical eigenvalues from linear stability theory have real parts of order 10^{-4}–10^{-6}.

As Fig. 3 and the results in Table 2 show the dependence of the critical parameter on the Prandtl number is not linear at those points where the imaginary part of the eigenvalue is zero. The results of linear and energy theories for other Prandtl numbers are summarized in Figs. 4, 5 and Table 3.

In Figs. 3–5 the dependence of the critical value for both stability theories on the Prandtl number can be compared. In case of small Prandtl numbers a big region exists, which is open to subcritical instabilities. For big Prandtl numbers this region is smaller.

The calculations show that there is a big difference between critical numbers for energy and linear theories for small Prandtl numbers (the difference is 14% for $Pr = 0.28$). For large Prandtl numbers this difference decreases (2% for $Pr = 100$). This difference is less for

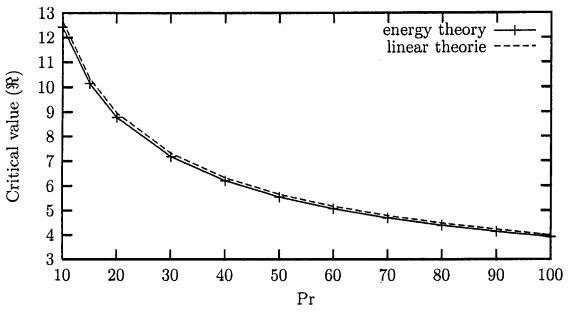

Fig. 4. Stability curve for large Pr and $\eta = 0.9$.

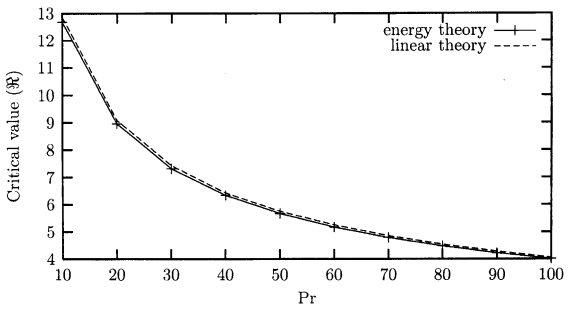

Fig. 5. Stability curve for large Pr and $\eta = 0.925$.

Table 4
Dependence of the critical stability parameters on wave number m

m	$\eta = 0.9$				$\eta = 0.925$			
	$Pr = 0.1$		$Pr = 0.7$		$Pr = 0.1$		$Pr = 0.7$	
	$\Re_{cE}$	$\Re_{cL}$	$\Re_{cE}$	$\Re_{cL}$	$\Re_{cE}$	$\Re_{cL}$	$\Re_{cE}$	$\Re_{cL}$
0	71.47	94.606	46.87	48.197	71.28	91.728	47.79	48.814
1	71.49	94.63	46.89	48.2	71.29	91.74	47.80	48.815
2	71.53	94.73	46.91	48.25	71.31	91.80	47.82	48.84
3	71.61	94.92	46.99	48.32	71.36	91.90	47.85	48.88
4	71.72	95.17	47.1	48.42	71.42	92.03	47.90	48.94

narrow shells. The best λ number decreases with increasing of Pr and ϵ. For narrow gaps the critical Rayleigh numbers are very close to 1708. The dependence of the critical value on Prandtl number for energy stability theory is linear for small Prandtl numbers and is not linear for large Prandtl numbers.

7. Conclusions

The goal of this research was the calculation of the lower stability limit for the natural convection between spherical shells with energy stability method and comparison of these results with linear stability theory. The calculations were made for large range Prandtl number and for different radius ratios. This investigation was made for narrow gaps.

The investigation shows that the difference between the linear and energy stability analyses is larger for small Prandtl numbers than for large Prandtl numbers.

In the future research the stability results should be extended to the range of smaller radius ratios and compared with experimental results.

Acknowledgements

This work was supported by BEOS – Bremer Engineering Operation Systems. One of us (V.T.) would like to acknowledge many useful discussions with Dipl.-Phys. W. Brasch, Dipl.-Phys. M. Junk and Dipl.-Phys. B. Sitte.

References

[1] B.R. Munson, D.D. Joseph, Viscous incompressible flow between concentric rotating spheres. Part 2. Hydrodynamic stability, J. Fluid Mech. 49 (1971) 305–318.
[2] B.R. Munson, M. Menguturk, Viscous incompressible flow between concentric rotating spheres. Part 3. Linear stability and experiments, J. Fluid Mech. 69 (1975) 705–719.
[3] F.H. Busse, Patterns of convection in spherical shells, J. Fluid Mech. 72 (1975) 65–85.
[4] F.H. Busse, N. Riahi, Patterns of convection in spherical shells. Part 2, J. Fluid Mech. 123 (1982) 283–301.
[5] D.D. Joseph, C.C. Shir, Subcritical convective instability. Part 1. Fluid layers, J. Fluid Mech. 26 (1966) 753.
[6] D.D. Joseph, S. Carmi, Subcritical convective instability. Part 2. Spherical shells, J. Fluid Mech. 26 (1966) 769.
[7] S. Chandrasekhar, Hydrodynamic and Hydromagnetic Stability, Oxford University Press, Oxford, 1961.
[8] S.H. Yin, R.E. Powe, J.A. Scanlan, E.H. Bishop, Natural convection flow patterns in spherical annuli, Int. J. Heat Mass Transfer 16 (1973) 1785–1795.
[9] A. Brucks, Untersuchungen zur thermischen Konvektion im weiten Kugelspalt mit und ohne Rotation, Diploma Thesis, ZARM, University of Bremen, 2000.
[10] M.T. Farmer, R.W. Douglas, S.A. Trogdon, The stability of natural convection in narrow-gap spherical annuli to axisymmetric disturbances, Int. J. Heat Mass Transfer 29 (1986) 1575–1584.
[11] J.L. Wright, R.W. Douglas, Natural convection in narrow-gap spherical annuli, Int. J. Heat Mass Transfer 29 (1986) 725–739.
[12] D.R. Gardner, Linear stability and bifurcation of natural convection flows in narrow-gap, concentric spherical annulus enclosures, Ph.D. thesis, University of Nebraska-Lincoln, Lincoln, Nebraska, 1988.
[13] R.W. Douglass, K.G. TeBeest, S.A. Trogdon, D.R. Gardner, Prandtl number effects on the stability of natural convection between spherical shells, Int. J. Heat Mass Transfer 33 (1990) 2533–2544.
[14] J. Serrin, On the stability of viscous fluid motions, Arch. Rational Mech. Anal. 3 (1959) 1.
[15] D.D. Joseph, in: Stability of Fluid Motions I & II, vol. 27, Springer, Berlin, 1976, p. 28.
[16] A. Zebib, A Chebyshev method for the solution of boundary value problems, J. Comp. Phys. 53 (1984) 443–455.